Switching of the magnetic interactions from antiferromagnetic to ferromagnetic in the heavy-fermion compound $CeRu_2Si_2$ under high magnetic field

1998 J. Phys.: Condens. Matter 10 2363

(http://iopscience.iop.org/0953-8984/10/11/002)

J. Phys.: Condens. Matter **10** (1998) 2363–2373. Printed in the UK PII: S0953-8984(98)89202-3

Switching of the magnetic interactions from antiferromagnetic to ferromagnetic in the heavy-fermion compound $CeRu_2Si_2$ under high magnetic field

S Raymond†‡, L P Regnault†, S Kambe†, J Flouquet† and P Lejay§

† CEA-Grenoble, Département de Recherche Fondamentale sur la Matière Condensée, SPSMS/MDN, 38 054 Grenoble Cédex 9, France

‡ Brookhaven National Laboratory, Physics Department, Upton, NY 11973, USA

§ Centre de Recherche sur les Très Basses Températures, CNRS BP 166, 38 042 Grenoble Cédex 9, France

Received 13 November 1997

Abstract. Inelastic neutron scattering studies of $CeRu_2Si_2$ under high magnetic field are reported. The dynamic short-range antiferromagnetic correlations are progressively replaced by static long-range ferromagnetic order when the field is increased. A simple interpretation using a phenomenological model leads to the conclusion that the exchange interactions are field dependent and that their weight is shifted from the antiferromagnetic point to the ferromagnetic point as the field changes.

1. Introduction

Heavy-fermion (HF) compounds are anomalous cerium- or uranium-based intermetallic compounds driven to magnetic instability as a result of the competition between the Kondo effect and the RKKY interactions. These interactions, oscillating in nature, give rise to either ferromagnetic or antiferromagnetic bonds between magnetic atoms. Usually the ground state is close to antiferromagnetic order, which favours the HF phenomenon. A magnetic quantum critical point is expected at the magnetic–non-magnetic boundary for a critical value r_c of a control parameter (either pressure, P_c, or concentration, x_c, for alloyed compounds). Experimentally, near this theoretical boundary, the available compounds exhibit a wide range of ground states, varying from conventional magnets with strong local fluctuations to Pauli paramagnets with dynamical antiferromagnetic correlations [1, 2]. $CeRu_2Si_2$ is a Pauli paramagnet, without any magnetic ordering down to 30 mK. It is characterized by a rather large linear coefficient of the specific heat, $\gamma = 350$ mJ mol^{-1} K^{-2}, below 1 K [3]. This compound crystallizes in the $I4/mmm$ tetragonal space group with the $ThCr_2Si_2$ structure and the lattice parameters $a = b = 4.197$ Å and $c = 9.797$ Å [4]. At low temperatures, a sharp inflection point appears in the magnetization curves for the field $H_m = 7.7$ T applied along the tetragonal c-axis. This so-called pseudometamagnetic transition is indicative of the strong interplay between the magnetism and the electronic and lattice properties. Below 1 K, the magnetic susceptibility, the linear temperature coefficient (γ) of the specific heat, the quadratic temperature term of the resistivity, the derivative of the magnetostriction and the longitudinal sound velocity exhibit sharp peaks at H_m [3, 5]. Inelastic neutron scattering (INS) experiments [6–7] show that the inelastic magnetic signal

0953-8984/98/112363+11$19.50

peaks at the incommensurate wave vectors $\boldsymbol{k}_1 = (0.31, 0, 0)$ and $\boldsymbol{k}_2 = (0.31, 0.31, 0)$ and disappears at the transition. Some recent work has dealt with the nature of the 4f electrons on either side of H_m. Large changes of the Fermi surface, measured by the de Haas–van Alphen technique, were interpreted as the signature of the change of the 4f electrons from itinerant to localized at the metamagnetic transition [8]. It becomes apparent however, when making a comparison with specific heat measurements, that some electronic orbits are missing. Hall effect measurements [9] also show a continuous behaviour at the transition. NMR experiments performed under high magnetic field [10] were explained in terms of ferromagnetic fluctuations enhanced at the metamagnetic transition. Models dealing with the metamagnetic transition for this class of compounds often include ferromagnetic interactions [11–13]. On another hand, the dual model of heavy-fermion electrons [14–16] explains the metamagnetic transition in terms of a competition between the RKKY interaction of the localized part of the quasiparticles and the exchange interactions of the itinerant part. A parallel can be drawn with itinerant-electron metamagnetism, for which it is well known that some compounds are located near a ferromagnetic instability and that the Stoner criterion is almost satisfied in the paramagnetic phase, e.g. in YCo_2 [17]. A recent model [18] includes both a field-dependent exchange interaction and a Kondo-collapse volume effect. While the latter effect is well documented experimentally [3], the former was only qualitatively expected from INS measurements [6–7]. The purpose of this work was to study and compare the magnetic excitation spectrum below and above the pseudometamagnetic transition by means of INS and, hence, to reveal the nature of the 4f spin interactions.

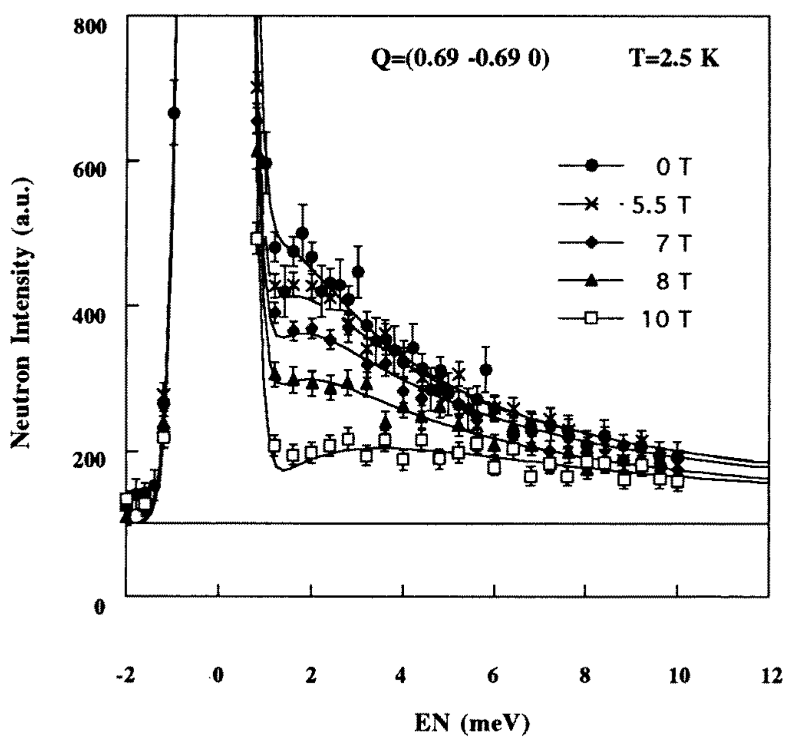

Figure 1. Energy scans performed at $\boldsymbol{Q} = (0.69, 0.69, 0)$ at 2.5 K at various fields on IN8 using configuration (a).

2. Experimental conditions

The INS experiments were performed at the ILL high-flux reactor on the triple-axis spectrometers IN8 (thermal source) and IN12 (cold guide). Many experimental configurations were used in order to cover a wide range of experimental resolutions. Configuration (a) corresponds to the work performed on IN8. The fixed-final-momentum mode was chosen, using $k_F = 2.662$ Å^{-1}. A pyrolytic graphite filter placed after the sample was used in order to reduce higher-order contamination. The collimations were 60′–sample–60′–60′. The analyser was slightly horizontally curved. Configurations (b) and (c) correspond to work performed on IN12 respectively in the constant-final-momentum mode using $k_F = 1.97$ Å^{-1} and in the constant-initial-momentum mode with $k_I = 1.5$ Å^{-1}. In each configuration a beryllium filter was used on the scattered beam (or incident beam) to reduce the higher-order contamination. The collimations were 60′–sample–60′–60′. On both spectrometers the [002] reflection of pyrolytic graphite was used for the monochromator and the analyser. The crystal was grown by the Czochralsky method [19] and had a typical size of 500 mm^3. On each spectrometer, it was mounted in the 12 T vertical cryomagnet of CEA-Grenoble. The horizontal scattering plane was the (a, b) plane of the crystal and the field was applied along the easy tetragonal c-axis. Compared to previous experiments performed on IN8 with the same crystal [6–7], the combined use of a new small-gap cryomagnet (with thinner aluminium screens) and a vertically focusing monochromator, and a slightly horizontally curved analyser give rise to a gain by a factor of 2 in the counting rate.

3. The disappearance of the antiferromagnetic correlations

Previous studies of the magnetic excitation spectrum of $CeRu_2Si_2$ under high magnetic field focused on the disappearance of the signal at the vectors $\boldsymbol{k}_1$ and $\boldsymbol{k}_2$ [6–7]. This work extends the measurements of the magnetic excitation spectrum to a larger area of the Brillouin zone in order to study the transfer of spectral weight from the incommensurate points to the ferromagnetic point versus the magnetic field. Preliminary studies showed that the behaviour is essentially the same for the two wave vectors $\boldsymbol{k}_1$ and $\boldsymbol{k}_2$. In this study, data are mainly taken around the point $\boldsymbol{k}_2$. The main feature already known about is shown in figure 1, which represents a constant-$\boldsymbol{Q}$ scan at $\boldsymbol{Q} = \boldsymbol{k}_2$ and $T = 2.5$ K for magnetic fields of 0, 5.5, 7, 8 and 10 T. The magnetic excitation spectrum around this vector, characterized by a spin-fluctuation lineshape, vanishes when the field is increased. In addition, constant-E scans performed at $E = 1.6$ meV are shown in figure 2. This is the first time that such scans have been performed under magnetic field, the previous studies stressing only the energy response. The main feature is the broadening of the wave-vector response. Within the accuracy of our data we do not see a shift of the peak position when the field is increased. The maximum intensity occurs at $q = 0.73$ rather than at the expected value $q = 0.69$. We ascribe this difference to focusing effects and this may also have been observed by another group [20]. In order to analyse our data around the wave vector $\boldsymbol{k}_2$ (this instability wave vector will be denoted as $\boldsymbol{k}$ in the following), we write the intensity as $I(\boldsymbol{Q}, \omega) = I_{bg} + (1 + n(\omega))\chi''(\boldsymbol{Q}, \omega)$, where I_{bg} is the neutron background, assumed to be constant and determined at negative energy transfer, and $n(\omega)$ is the Bose factor. For each scan, a one-dimensional convolution in the direction of the running variable was applied. Without any model to guide us, we chose the simplest form for the dynamical susceptibility,

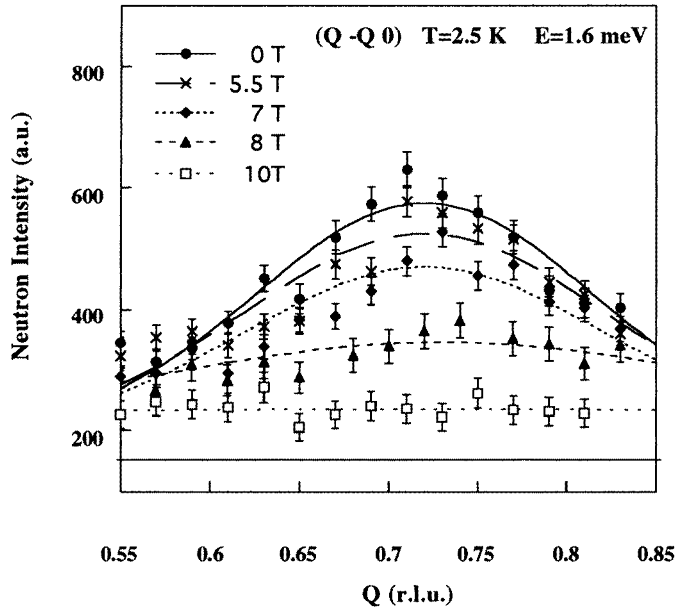

Figure 2. $\boldsymbol{Q}$-scans performed at 2.5 K at $E = 1.6$ meV at various magnetic fields on IN8 using configuration (a).

namely a Lorentzian lineshape:

$$\chi''(\boldsymbol{Q}, \omega) = \frac{\chi_Q \omega \Gamma_Q}{\omega^2 + \Gamma_Q^2}. \tag{1}$$

Beside the incoherent signal, only two parameters are fitted in a constant-$\boldsymbol{Q}$ scan: the susceptibility χ_Q and the energy width Γ_Q. The parameters extracted for $\boldsymbol{Q} = \boldsymbol{k}$ from this fit are shown in figures 3(a) and 3(b). It appears to be in accordance with a rough examination of the data that the susceptibility χ_k decreases much more than the energy width increases with the magnetic field. It follows that the product $\chi_k \Gamma_k$ decreases when the magnetic field is increased. In the low-field region ($H < 5$ T), there is a plateau in the susceptibility followed by a significant drop for higher magnetic fields. As regards the analysis of the constant-E scans, the energy width Γ_Q is expanded as $\Gamma_Q = \Gamma_k + \alpha q^2$ ($\boldsymbol{q} = \boldsymbol{Q} - \boldsymbol{k}$). This allows us to extract a characteristic length $\xi = \sqrt{(\alpha/\Gamma_k)}$ whose field variation is shown in figure 3(c). This quantity decreases with the magnetic field, implying a shortening of the correlation length from that of two correlated moments in zero field to that of completely uncorrelated moments at 10 T. At this highest field, the signal is almost flat in the $\boldsymbol{Q}$-range shown in figure 2 for the energy transfer of 1.6 meV, but it is slightly peaked when this range is extended over all of the Brillouin zone and especially for higher constant-energy transfer. This means that unlike our characteristic length, the true correlation length does not vanish for a field of 10 T. In particular, this remaining signal almost disappears around the ferromagnetic point $\boldsymbol{Q} = (1, 1, 0)$. This is inconsistent with a separate single-site (i.e. truly $\boldsymbol{Q}$-independent) contribution. Consequently, in this paper, we analysed our data in a different way from that adopted in previous studies [6, 7]. In particular, the cross section can equally well be described, after considering the resolution of this experiment (using configuration (a)), with just one Lorentzian lineshape, whereas two

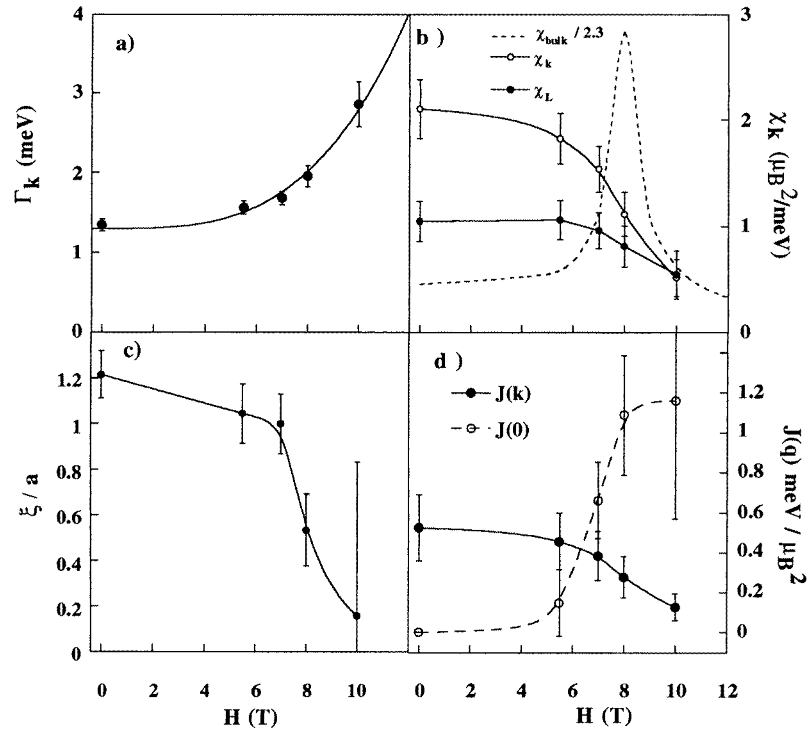

Figure 3. (a) The field variation of the energy width extracted from the fit to the data of figure 1 of cross section (1). The line is a guide for the eyes. (b) The field variation of the staggered susceptibility extracted from the data of figure 1. The local susceptibility is extracted from a simple model described in the text and the bulk susceptibilities are reproduced from [5]. Lines are guides to the eyes. (c) The field variation of the q-width extracted from a fit to the data of figure 2. The line is a guide for the eyes. (d) The field variation of the exchange coupling derived using a simple model described in the text.

Lorentzians were used in [6, 7], reflecting local fluctuations and correlated fluctuations. The second Lorentzian was modified and included an inelasticity, ω_0. While this early analysis gave a very accurate description of the data, linking it to a model is difficult. We choose a simpler analysis that allows a connection (made below) with microscopic parameters to be established. This description was also recently discussed and successfully applied in the study of the dynamics of the compounds $Ce_{0.925}La_{0.075}Ru_2Si_2$ and the comparison with macroscopic measurements [21]. INS data for the heavy-fermion compound $CeCu_6$ under a magnetic field were also analysed this way [22]. This latter compound undergoes a weak metamagnetic transition at $H_m = 2$ T, shown for example in the derivative of the magnetization, while this quantity has a negative curvature versus the magnetic field. From the point of view of the spin dynamics, the main difference from our present result on $CeRu_2Si_2$ arises from the fact that $\chi_k\Gamma_k$ was found to be independent of the magnetic field for the former compound. In particular, this allowed the authors of [22] to describe their results using a simple Hamiltonian including both the Kondo effect and intersite coupling. In this model a singlet–triplet splitting is considered. A quadratic field dependence for Γ_k is inferred from the lifting of the triplet degeneracy by the magnetic field. A Lorentzian-like field dependence of χ_k follows from $\chi_k\Gamma_k = \text{constant}(H)$. The fact that a similar interpretation cannot be made for $CeRu_2Si_2$ may have its origin in the strong metamagnetic behaviour observed, which implies that a more sophisticated treatment of the coupling between the localized and the itinerant electrons in HF compounds is required.

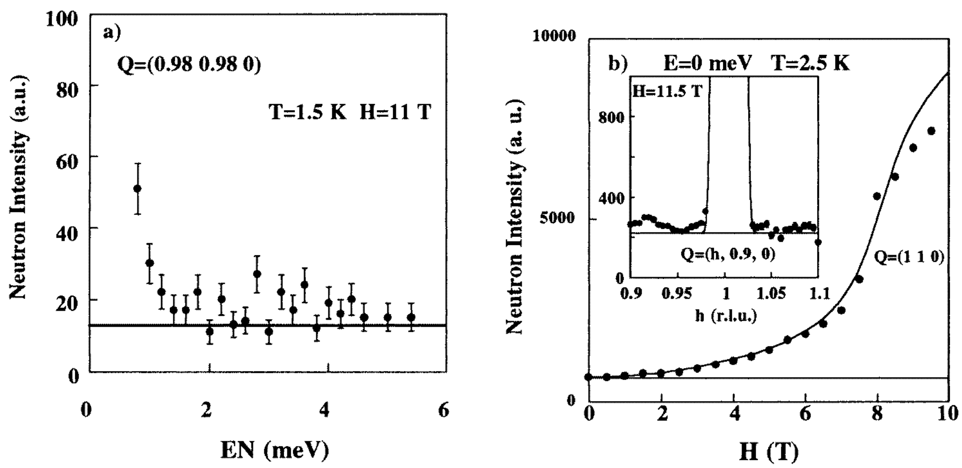

Figure 4. (a) An energy scan performed on IN12 with configuration (b) at 1.5 K and 11 T at $\boldsymbol{Q} = (0.98, 0.98, 0)$. (b) The variation of the maximum intensity at $\boldsymbol{Q} = (1, 1, 0)$ versus the field at 2.5 K. The line represents the square of the magnetization measured at 1.5 K [5] and rescaled. The inset shows the foot of the Bragg peak at 11 T.

4. Investigation of the ferromagnetic state

Systematic scans were performed around the ferromagnetic zone centre under high magnetic field. No excitations were found up to 10 meV near the (110) zone centre. In the space group $I4/mmm$, the magnetic cerium atoms form a Bravais lattice. As a consequence there is no structure factor and each Bragg peak is equivalent as regards magnetic scattering. Nevertheless, we choose (110) because it is a weak nuclear peak. The configurations used were (a), (b) and (c), giving total energy widths of the incoherent signal of 0.9, 0.4 and 0.2 meV respectively. This means that a quasielastic signal with a width of the order of half the best resolution, say 0.1 meV, can be detected. This is our instrumental limit dividing a phenomenon which will be seen as static from a phenomenon which will be seen as dynamic. The strong Bragg peak at this position probably increases this limit. Systematic scans were performed probing the energy window allowed by each configuration. No significant signal was detected—neither on the low-energy side, unambiguously down to 0.4 meV, nor on the high-energy side up to 10 meV. For example, a scan performed at $\boldsymbol{Q} = (0.98, 0.98, 0)$ with the configuration (b), suitable for studying the range 1–5 meV, is shown in figure 4(a). We thus conclude that in the range 0.4–10 meV, covering cold- and thermal-neutron scattering, no magnetic excitation characteristic of the ferromagnetic zone centre is observed. In addition, the Bragg peak lineshape was studied. When the spectrometer is set at zero energy transfer, the peak intensity measured at $\boldsymbol{Q} = (1, 1, 0)$ shows a strong non-linearity characteristic of the metamagnetic transition. This is shown in figure 4(b), with a shape consistent with that for the bulk magnetization measurements, which are reproduced for comparison [5]. The discrepancy at high field is due to the difference between the temperatures at which the two measurements were performed. Extinction corrections may also be partially responsible for this discrepancy when the signal becomes stronger at high magnetic field. As shown in the inset of figure 4(b), no wings are observed beyond some statistical noise in the tails of this Bragg peak for wave vectors slightly shifted from the centre of the zone at 11.5 T. The same is true at 8 T, where the fluctuations may be expected to reach a maximum as in real second-order phase transitions. This rules out the occurrence of short-range fluctuations and, consequently, the ferromagnetic magnetic-field-induced order is long range. This fact, associated with the absence of low-energy inelastic excitation, leads us to the conclusion that the 4f response probed by our technique is static and is characteristic of a long-range field-induced order.

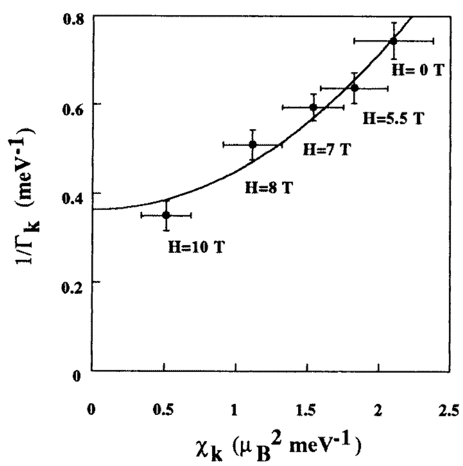

Figure 5. A plot of the energy width Γ_k of the constant-$\boldsymbol{Q}$ spectra versus the susceptibility χ_k for various fields. The line is a quadratic fit to the model described in the text.

5. Discussion

5.1. The competition between antiferromagnetic and ferromagnetic interactions

From our phenomenological parameters χ_k, and Γ_k, microscopic parameters can be deduced. The magnetic excitation spectrum can be interpreted within the random-phase approximation (RPA) as previously proposed by Kuramoto [14] and Moriya and co-workers [2] for HF compounds. In this picture, a local dynamical susceptibility mainly controlled by the Kondo interaction is enhanced by RKKY interactions $J(\boldsymbol{Q})$. The total susceptibility of the system is written as

$$\chi(\boldsymbol{Q},\omega) = \frac{\chi_L(\omega)}{1 - J(\boldsymbol{Q})\chi_L(\omega)} \tag{2}$$

where the local dynamical susceptibility is approximated by a Lorentzian with two parameters, a local susceptibility χ_L and a characteristic local energy Γ_L:

$$\chi_L(\omega) = \frac{\chi_L}{1 - \mathrm{i}\omega/\Gamma_L}. \tag{3}$$

It follows that the parameters used in the imaginary part of the susceptibility (1) are related to this new set of parameters via

$$\Gamma_Q = \Gamma_L(1 - J(\boldsymbol{Q})\chi_L) \tag{4}$$

$$\chi_Q = \frac{\chi_L}{1 - J(\boldsymbol{Q})\chi_L}. \tag{5}$$

For each magnetic field, the relation $\chi_Q\Gamma_Q = \chi_L\Gamma_L$ holds. Taking the above expressions as phenomenological, we want to study the field dependence of the physical quantities $J(\boldsymbol{Q})$, χ_L and Γ_L. To extract three quantities from two previously fitted quantities at $Q = k$, some assumptions are needed. For this purpose, it is useful to recast our results in the form

$$\frac{1}{\Gamma_k} = \frac{1}{\Gamma_L}(1 + J(\boldsymbol{k})\chi_k). \tag{6}$$

$1/\Gamma_k$ is plotted versus χ_k in figure 5. A phenomenological line is needed for extracting the microscopic parameter $J(\boldsymbol{k})$. Among many possibilities, a model starting with the following two hypotheses was chosen.

(1) Γ_L is considered to be field independent, since the effects of the magnetic field are much more important for χ_k than for Γ_k (and correspondingly, are more important for χ_L than for Γ_L).

(2) $J(\boldsymbol{k})$ goes to zero for very large magnetic fields, which is supported by the predominantly RKKY nature of these interactions.

We then make a Taylor expansion of $1/\Gamma_k$ in terms of χ_k which leads, after identification with (6), to $\Gamma_L = 2.8$ (0.2) meV and to the link between $J(\boldsymbol{k})$ and χ_k: $J(\boldsymbol{k}) \approx 0.25\chi_k$. This relation is related to the fact that the RKKY exchange parameter is proportional to the conduction electron susceptibility. The proportionality between the conduction electron susceptibility and the 4f susceptibility is not obvious but was mentioned in a study of the magnetic ordering of $Ce(Ru_{1-x}Rh_x)_2Si_2$ [23]. Other phenomenological approaches can be considered. However, a simpler one based on a linear line, which could fit the data of figure 5 just as well, would lead to assumptions that are unphysical, unlike hypotheses (1) and (2). The exchange parameter at $q = 0$ is extracted in the same spirit. The hypothesis is here that $J(0) \approx 0$ for $H = 0$, which is related to the fact that no magnetic interaction has been observed so far at $q = 0$. With these assumptions, we have $\chi_{\mathrm{bulk}} = \chi_L$ at zero field. This relation is also used in order to normalize our neutron intensity. The parameter $J(0)$ is then deduced by inverting (5) knowing the field dependence of χ_L (this work) and χ_{bulk} [5]. The decrease of the local susceptibility χ_L with the field is shown in figure 3(b) together with the results of the bulk measurements and χ_k. It implies that the ferromagnetic coupling must increase drastically with the field. The value of the exchange parameter $J(0)$ deduced is shown in figure 3(d), together with $J(\boldsymbol{k})$ for comparison. Not surprisingly, the curves representing these two quantities cross at around H_m. Taking the value of the Ce moment to be of the order of 1.5 μ_B† (deduced from the magnetization under high magnetic field), the Zeeman energy associated with H_m is 1 meV. With this simple model, we find $J(q = 0, H = H_m) \approx J(q = k, H = H_m) \approx \mu H_m \approx \Gamma_L/2$. The factor 2 difference between the exchange parameters and the Kondo-like energy scale Γ_L may arise from our simple model or may be intrinsic (various measurements lead to an estimate of T_K in the range 10–30 K). In this picture the exchange parameters have to be field dependent, because the local susceptibility decreases with the field when the

† In a previous paper [21], the (inappropriate) free-Ce-ion moment was used, leading to different exchange parameters.

bulk susceptibility increases at the same time. Most often, magnetic ordering occurs through an instability in the non-interacting susceptibility and not through a variation of the exchange interactions. This mechanism is not relevant in the case studied here, where the local susceptibility decreases with the field in accordance with a simple Kondo model. Similarly to our study, reference [24] reported temperature-dependent exchange coupling for the antiferromagnetic heavy-fermion U_2Zn_{17}. To explain this peculiarity, it was proposed that in the dual model of the heavy-fermion compound [14–16] $J(\boldsymbol{Q})$ is in fact an effective coupling which includes both the RKKY interaction between the localized component and the polarization function of the itinerant component. The metamagnetic transition of $CeRu_2Si_2$ and UPt_3 was also described by the authors of [14–16] in this spirit. In the model of Satoh and Ohkawa [18], a field-dependent interaction reaching its maximum value at H_m is considered. This reflects the evolution under a magnetic field of the camel-back structure assumed for the electronic density of states. This field dependence, although different from that of $J(0)$ in our model, is an important improvement on the theoretical work done so far, and is qualitatively in agreement with our findings. Although our simple model may not be the only one that can be used to describe the data, it shows unambiguously that the decrease of the antiferromagnetic correlations leads to a non-linear increase of the $q = 0$ component. This conclusion was found to be robust when tested using some other models.

5.2. Static versus dynamic order above H_m

At the highest magnetic fields, the response probed by means of INS in this study is static and is characteristic of induced magnetic ordering. Experimentally, it was shown by means of an NMR study of the Si sites [10] that both of the inverse spin-relaxation times, $1/T_1$ and $1/T_2$, are enhanced at the metamagnetic transition, the second one showing a much more significant increase. The stronger enhancement observed for $1/T_2$ was interpreted as reflecting longitudinal ferromagnetic fluctuations along the tetragonal axis. On the other hand, since the INS experiments probe the dynamical susceptibility $\chi''(\boldsymbol{Q}, \omega)$ in the range of $\boldsymbol{Q}$ corresponding to the 4f response (near the Bragg peak $\boldsymbol{Q} = (1, 1, 0)$, the form factor of the magnetization density is mainly characteristic of 4f electrons and all of the other contributions are small [25]) and in the range of energy 0.4–10 meV studied in this work. Our results show that the ferromagnetic dynamic fluctuations probed by means of NMR appear to be static in the neutron scattering study. Very-low-energy studies are needed for a better comparison. Due to kinematical constraints, only studies of the scattering near the forward direction can achieve a good resolution. In this area of the reciprocal space, not only is the 4f response probed but so also is the response from 3d orbitals. This kind of experiment was performed on UPt_3 [26] and interpreted within the framework of the Fermi liquid theory. In the comparison between the NMR and INS results, a difficulty arises from the fact that the NMR probes the Si sites and the neutron scattering probes the 4f sites. But, experimentally and theoretically [27], it is known that the conduction electron relaxation rate reflects to some extent the f-electron susceptibility. Finally, transverse fluctuations (spin-wave like) are not likely to occur at low energies due to the strong magnetocrystalline anisotropy which leads to a nearly pure $|\pm 5/2\rangle$ ground state. The splitting between the lowest CEF doublets is of the order of 220 K = 19 meV [28] as estimated from specific heat measurements. On the another hand, CEF excitations were not observed in the INS studies of this compound [29]. In any case, this energy scale is not relevant for the mechanism of the metamagnetic transition, which involves low-lying excitations.

6. Conclusion

Our study of the magnetic excitation spectrum of $CeRu_2Si_2$ under a magnetic field shows that while the short-range dynamic antiferromagnetic correlations disappear at the incommensurate wave vector, long-range static ferromagnetic order appears at $q = 0$. At the same time, the antiferromagnetic exchange parameter $J(\boldsymbol{k})$ is superseded by the ferromagnetic coupling $J(0)$. The existence of competing ferromagnetic and antiferromagnetic interactions reaching a critical value at the metamagnetic transition in $CeRu_2Si_2$ may be a feature common to HF compounds. In this respect, studies on the ferromagnetic compound $CeRu_2Ge_2$ ($T_c \approx 10$ K) are under consideration. This compound, when doped with Si, exhibits a double transition from the paramagnetic to an antiferromagnetic state and finally to a ferromagnetic state on cooling. As for $CeRu_2Si_2$, this leads to the question of the possible coexistence of two nearly degenerate antiferromagnetic and ferromagnetic ground states. An important issue will be that of establishing whether, for this latter compound, the magnetic quantum critical point between the long-range magnetic ordered state and the paramagnetic state can be reached directly through a ferromagnetic–paramagnetic transition or whether it must be preceded by a ferromagnetic–antiferromagnetic transition.

Acknowledgments

We thank J Bossy for his help during the experiment on IN8 and B Fåk for his help with the work on IN12 and stimulating discussions. Some of the data were analysed during a stay at BNL in the neutron scattering group. One of us (SR) thanks S M Shapiro for useful discussions. Part of this work was supported by the Division of Materials Sciences, US DOE, under contract No DE-AC0276CH00016.

References

[1] For a review of experimental work, see e.g.
Steglich F 1991 *J. Magn. Magn. Mater.* **100** 186
de Visser A and Franse J J M 1991 *J. Magn. Magn. Mater.* **100** 204
[2] For theoretical guidelines, see
Millis A J 1993 *Phys. Rev.* B **48** 7183
Moriya T and Takimoto T 1995 *J. Phys. Soc. Japan* **64** 960
[3] Flouquet J, Kambe S, Regnault L P, Haen P, Brison J P, Lapierre F and Lejay P 1995 *Physica* B **215** 77 and references therein
[4] Hiebl K, Howath C, Rogl P and Sienko M 1983 *J. Magn. Magn. Mater.* **37** 287
[5] Haen P, Flouquet J, Lapierre F, Lejay P and Remenyi G 1987 *J. Low Temp. Phys.* **67** 391
[6] Jacoud J L, Regnault L P, Rossat-Mignod J, Vettier C, Lejay P and Flouquet J 1989 *Physica* B **156+157** 818
[7] Rossat-Mignod J, Regnault L P, Jacoud J L, Vettier C, Lejay P, Flouquet J, Walker E, Jaccard D and Amato C 1988 *J. Magn. Magn. Mater.* **76+77** 376
[8] Aoki H, Uji S, Albessard A K and Onuki Y 1993 *Phys. Rev. Lett.* **71** 2110
[9] Kambe S, Flouquet J, Haen P and Lejay P 1996 *J. Low Temp. Phys.* **102** 477
[10] Tagaki S, Ohama T and Onuki Y 1994 *ISSP, Tokyo, Report*
[11] Brenig W 1987 *Solid State Commun.* **64** 203
[12] Ohkawa F J 1989 *Solid State Commun.* **71** 907
[13] Ueda K, Yamamoto K and Konno R 1990 *J. Magn. Magn. Mater.* **90+91** 419
[14] Kuramoto Y 1989 *Physica* B **156+157** 789
[15] Kuramoto Y and Miyake K 1990 *J. Phys. Soc. Japan* **59** 2831
[16] Miyake K and Kuramoto Y 1990 *J. Magn. Magn. Mater.* **90+91** 438
[17] Steiner W 1979 *J. Magn. Magn. Mater.* **14** 47
[18] Satoh H and Ohkawa F 1998 *Preprint*
[19] Lejay P, Muller J and Argoud R 1993 *J. Cryst. Growth* **130** 238

[20] Kadowaki H 1996 private communication
[21] Raymond S, Regnault L P, Kambe S, Mignot J M, Lejay P and Flouquet J 1997 *J. Low Temp. Phys.* **109** 205
[22] Aeppli G, Yoshizawa H, Endoh Y, Bucher E, Hufnagl J, Onuki Y and Komatsubara T 1986 *Phys. Rev. Lett.* **57** 122
[23] Kawarazaki S, Sato M, Kadowaki H, Yamamoto Y and Miyako Y 1997 *J. Phys. Soc. Japan* **66** 2473
[24] Broholm C, Kjems J K, Aeppli G, Fisk Z, Smith J L, Shapiro S M, Shirane G and Ott H R 1987 *Phys. Rev. Lett.* **58** 917
[25] Form factor measurements are in progress.
[26] Bernhoft N and Lonzarich J L 1995 *J. Phys.: Condens. Matter* **7** 7325
[27] Evans S M and Coqblin B 1991 *Phys. Rev.* B **43** 12 790
[28] Lehmann P 1987 *PhD Thesis* Strasbourg University
[29] Severing A, Holland-Moritz E, Rainford B D, Culverhouse S R and Frick B 1989 *Phys. Rev.* B **39** 2557